

B.Z. Polvonov<sup>1\*</sup>, Yu.I. Gafurov<sup>1</sup>, U.A. Otajonov<sup>1</sup>,  
M.X. Nasirov<sup>2</sup>, B.B. Zaylobiddinov<sup>3</sup>

<sup>1</sup>Ferghana branch of Tashkent University of Information Technologies, Ferghana, Uzbekistan

<sup>2</sup>Ferghana Polytechnic Institute, Ferghana, Uzbekistan

<sup>3</sup>Branch of National Research Nuclear University “MEPHI” in Tashkent city, Tashkent, Uzbekistan

\*e-mail: bakhtiyor@mail.ru

(Received 7 October 2022; accepted 15 December 2022)

### The specificity of photoluminescence n-CdS/p-CdTe in semiconductor heterostructures

**Abstract.** The low-temperature (4.2 K) near-band-edge photoluminescence spectrum of a thin fine-grained ( $h$ ,  $d_{gr} \leq 1 \mu\text{m}$ ) polycrystalline CdTe layer in an n-CdS/p-CdTe film heterostructure subjected to frontal excitation by an Ar<sup>+</sup> laser with an intensity of  $\sim 44 \text{ W/cm}^2$  consists of a dominant intrinsic (e-h) emission band with a half-width  $\Delta_A = 10\text{--}12 \text{ meV}$  and a blue shift  $\Delta E_r \approx 25 \text{ meV}$  of the red edge with respect to  $E_g$ , its LO+nLA phonon replica ( $\Delta_B \approx 40 \text{ meV}$ ) with a weak doublet structure, and a wide ( $\Delta_D \approx 100 \text{ meV}$ ) surface-interface luminescence band peaking at a frequency  $\hbar\omega \approx 1.49 \text{ eV}$ . Rear-side illumination of the photoresistive CdS layer in the intrinsic absorption range with an intensity  $L_{\text{ill}} \approx 5 \cdot 10^2 \text{ lx}$  almost completely destroys the e-h band and all related luminescence lines, which are replaced with an asymmetric polariton emission doublet having an exciton resonance frequency  $\hbar\omega \approx 1.59 \text{ eV}$  ( $\Delta_{\text{ex}} \approx 25 \text{ meV}$ ) and a wide line of shallow donor–acceptor pairs ( $\Delta_{\text{DAP}} \approx 40 \text{ meV}$ ) at a frequency of  $\hbar\omega \approx 1.54 \text{ eV}$ , whose maximum intensity is almost two orders of magnitude lower than that of the A line in the absence of illumination.

**Keywords:** photoluminescence, intensity, exciton, polariton, resonance, frequency, asymmetric, emission band.

#### Introduction

Low-temperature photoluminescence (LTPL) spectroscopy is a rapid nondestructive method for studying the electronic, optical, and photoelectric parameters of polycrystalline semiconductor film structures having photovoltaic properties [1–3]. Recently this technique has successfully been applied in fine studies of the characteristics of thin-film n-CdS/p-CdTe heterojunctions in solar cells, which were aimed at increasing the efficiency and improving the fabrication technology of the cells [4–8] (the polycrystalline p-CdTe film is the main absorbing layer in these structures). In particular, the LTPL spectra of the CdTe layer in a CdS/CdTe heterostructure (photocell with an efficiency of  $\sim 12\%$ ) in dependence of the laser excitation power and temperature were studied in [1–5].

The luminescence was found to shift to the red region of dominant impurity–defect emission at low excitation powers and be located mainly near the exciton emission edge at higher excitation

levels. Tuteja M. et al. [1], who used rear-side illumination by a He–Ne laser ( $\lambda = 0.6328 \mu\text{m}$ ) of a polycrystalline CdTe/CdS solar cell, observed three characteristic regions in the LTPL (10 K) spectra: (a) radiative transitions of bound excitons in the range from 1.58 to 1.60 eV, (b) a wide band of donor–acceptor pairs (DAPs) near 1.53 eV, and (c) a wide emission band of group defects with multiple phonon replicas in the range from 1.4 to 1.46 eV.

I. Caraman et al. [3] investigated the LTPL (78 K) spectra of thin (3–7  $\mu\text{m}$ ) CdTe films (both as-prepared and annealed in the presence of CdCl<sub>2</sub> saturated vapor) in a SnO<sub>2</sub>/CdS/CdTe/Ni solar cell upon excitation by He–Ne laser radiation with an intensity of  $\sim 12 \text{ kW/cm}^2$ . They showed that the illumination both from the side of the free CdTe surface and through the interface (heterojunction) gives rise to a wide impurity band peaking at 1.45 eV and a narrower band due to free (1.57–1.58 eV) and localized (1.558 eV) excitons. The exciton emission is barely present upon excitation through the interface, which is explained by the high

concentration of mechanical and structural defects in the latter. An analysis of the photoluminescence spectra made it possible to determine the spectrum of recombination levels and estimate the composition of the CdS<sub>x</sub>/CdTe<sub>1-x</sub> interface layer:  $x = 0.06$ .

Interface emission was also observed in other studies [4–7]. LTPL measurements [4, 5, 7] and LTPL study with electric-field modulation [6] proved the existence of a mixed crystalline CdS<sub>x</sub>Te<sub>1-x</sub> layer with a thickness of ~15 nm (with a low density of nonradiative recombination centers, the formation of which in the high-efficiency CdS/CdTe film solar cell is facilitated to a greater extent by the annealing in the presence of CdCl<sub>2</sub> vapor. The wide luminescence line at 1.42 eV is assigned to defect complexes involving the cadmium vacancy  $V_{Cd}$ , and the narrow line peaking at 1.59 eV is related to the exciton bound on the neutral acceptor [5-10].

In all the aforementioned studies, the thickness  $h$  of polycrystalline CdTe films and the crystallite sizes  $d_{cr}$  greatly exceeded the light wavelength  $\lambda$  in the luminescence spectral range under study. However, many recent studies (see, e.g., [8–10]) have shown thin-film  $n$ -CdS/ $p$ -CdTe heterostructures with characteristic sizes  $h, d_{cr} \sim \lambda$  to be promising elements for solar cells. In this case, thin fine-grained CdTe films obviously acquire properties of photonic microcrystals, the LTPL of which has barely been analyzed to date.

Recently we have investigated [11-14] the mechanisms of the formation of LTPL ( $T = 4.2$  K) spectra of thin ( $h \approx 0.5 - 0.8 \mu\text{m}$ ) polycrystalline pure CdTe films and indium-doped (CdTe:In) films, obtained by thermal vacuum deposition on glass substrates, in dependence of the presence of point and structural defects. It was shown that, in contrast to single crystals [12] and large-crystallite polycrystals [13, 15], the LTPL spectra of fine-grained ( $d_{cr} \leq 1 \mu\text{m}$ ) films do not exhibit any channels of exciton and DAPs emission. This is obviously caused by the following reasons. First, in the case under consideration, the crystallite size  $d_{cr}$  is on the same order of magnitude as the Debye screening length  $\ell_{Di} = \left( \frac{2\varepsilon\varepsilon_0\phi_i}{e^2|N_D - N_A|} \right)^{1/2}$  (where  $\varepsilon$  is the permittivity;  $\varepsilon_0$  is the permittivity of free space;  $e$  is the elementary charge;  $N_D$  and  $N_A$  are, respectively, the donor and acceptor concentrations; and  $\phi_i$  is the height of the surface potential barrier at the crystallite boundaries), and the contribution of the small quasi-neutral crystallite volume to the film LTPL is insignificant. Second, the surface potential barriers of crystallites

form internal built-in electrostatic fields in the space charge region (SCR), which leads to spatial separation of photogenerated electron–hole pairs in it and, correspondingly, generation of surface photovoltage and intrinsic luminescence (interbond  $e-h$  recombination), correlated by these pairs, of hot photocarriers under the condition

$$\tau_r \leq \tau_0, \tau_M \quad (1)$$

where  $\tau_r$ ,  $\tau_0$ , and  $\tau_M$  are, respectively, the radiative, nonradiative, and Maxwell lifetimes. Since the total lifetime of nonequilibrium electron is defined as

$$\frac{1}{\tau} = \frac{1}{\tau_r} + \frac{1}{\tau_0}, \frac{1}{\tau_0} = \frac{1}{\tau_{ex}} + \frac{1}{\tau_{DA}} + \frac{1}{\tau_M} + \frac{1}{\tau_p} + \dots, \quad (2)$$

are the electron relaxation times from this energy state with the formation of excitons and DAPs, respectively;  $\tau_p$  is the momentum relaxation time; etc., it is natural that, if the condition

$$\tau_r \ll \tau_{ex}, \tau_{DA} \quad (3)$$

is satisfied, the exciton and DAPs emission channels should be absent in the LTPL spectra in the first approximation; i.e., these channels remain experimentally unobserved against the strong background of the  $e-h$  luminescence. However, the situation changes when the condition

$$\tau_r \geq \tau_M \quad (4)$$

is implemented. The main mechanisms of photocarrier removal are nonradiative (e.g., electrical conductivity or surface recombination). Then the direct essential contribution of the radiative recombination of SCR-separated free electrons and holes to the LTPL is weakened, and one can observe weak exciton and DAPs lines in the spectra of thin fine-grained semiconductor films. Here, we propose a nontrivial method for implementing this possibility in an  $n$ -CdS/ $p$ -CdTe film heterostructure.

## Materials and Methods

The purpose of this study was to analyze the mechanisms of the formation of the edge photoluminescence spectrum of thin polycrystalline CdTe layer in an  $n$ -CdS/ $p$ -CdTe film heterostructure and develop a new optical photoelectric method for

detecting weak channels of exciton and DAPs emission. This approach makes it possible to investigate the interface composition and structure for nondestructive monitoring and diagnosing the properties of photovoltaic elements. We observed for the first time the build-up of exciton–polariton and shallow-Daps emission lines for the CdTe layer in the *n*-CdS/*p*-CdTe heterostructure, induced with the aid of additional illumination of the photoresistive CdS layer with intensity  $L_{ill} \approx 5 \cdot 10^2 \text{ lx}$ . It is believed that illumination of CdS reduces the shunting efficient of the CdTe resistance, weakening the heterojunction electric field and the corresponding exciton Stark effect [15] in the SCR surface crystallites. The Maxwell relaxation time  $\tau_M = \epsilon \epsilon_0 / \sigma_{ph}$  ( $\sigma_{ph}$  is the photoconductivity) of separated photocarriers in the CdTe crystallite volume decreases as well, due to which they leave no radiatively via surface interface levels or due to longitudinal photoconductivity before the radiative  $e-h$  recombination occurs ( $\tau_M < \tau_R$ ). Specifically this circumstance leads to quenching of all emission lines detected in the absence of illumination and build-up of free-exciton and shallow-DAP lines under additional illumination of the photoresistive CdS substrate.

## Results and Discussion

A sharp-interface *n*-CdS/*p*-CdTe film heterostructure (Figure 1) with an active absorbing *p*-CdTe layer was fabricated by thermal vacuum deposition on transparent glass substrate 1 in a unified technological cycle [16]. The lower photoresistive CdS layer (2) with an area of  $20 \times 5 \text{ mm}^2$  and thickness of  $0.2\text{--}0.4 \text{ }\mu\text{m}$  had an electronic conductivity. The multiplicity  $K = R_{dark} / R_{light}$  of the change in its resistance under illumination by a mercury lamp with  $L \approx 10^4 \text{ lx}$  reached  $\approx 10^2\text{--}10^3$  rel. units. According to the electron micrography data on the transverse cleavage and surface of the CdS film, the latter had columnar structure without pores, the crystallite sizes along the substrate surface turned out to be  $d_{cr} \approx 1\text{--}3 \text{ }\mu\text{m}$ . The upper *p*-CdTe layer (3) of thickness  $h = 0.5\text{--}0.8 \text{ }\mu\text{m}$  grew at a rate of  $1.5\text{--}2.0 \text{ }\text{\AA}/\text{s}$  at a substrate temperature  $T_s = 423\text{--}573 \text{ K}$  and had a fine-grained structure (crystallites of cubic modification with sizes  $d_{cr} \approx 0.8\text{--}1.0 \text{ }\mu\text{m}$ ). The active area of the *n*-CdS/*p*-CdTe heterostructure was  $70\text{--}80 \text{ mm}^2$ .

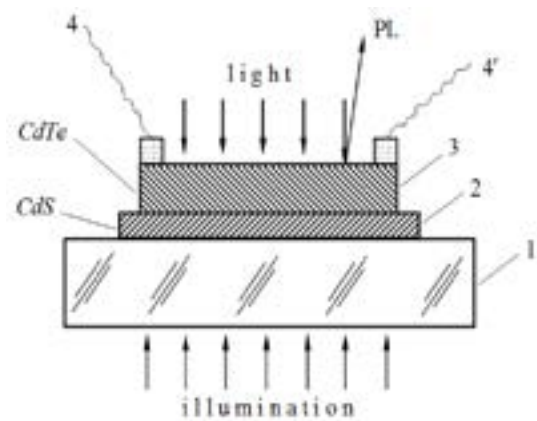


**Figure 1** – Schematic diagram of the photoluminescence excitation in the thin CdTe film ( $h_{Te} \approx 0.8 \text{ }\mu\text{m}$ ) of an *n*-CdS/*p*-CdTe heterostructure: (1) transparent glass substrate, (2) CdS photoresistive film ( $h_{CdS} \approx 0.3 \text{ }\mu\text{m}$ ), (3) photovoltaic layer (CdTe), and (4, 4') current-collecting ohmic contacts.

To measure the LTPL spectra, the *n*-CdS/*p*-CdTe film heterostructure was directly immersed in pumped liquid helium at a temperature of  $4.2 \text{ K}$ . Spectra were recorded on a setup based on a DFS-24 spectrometer, operating in the photon-counting mode at a minimum band gap of  $0.04 \text{ meV}$ . Frontal luminescence excitation (from the free-surface side) of the CdTe layer was performed at a wavelength  $\lambda = 476.5 \text{ nm}$  by an  $\text{Ar}^+$  laser beam focused on the CdTe layer surface into a spot  $0.4 \times 4 \text{ mm}$  in size; the laser power was  $\sim 7 \text{ mW}$ . The experiment was performed in the geometry of normal illumination and close-to-normal emission. The rear-side (through the glass substrate, see Figure 1) additional illumination of the CdS layer at different intensities was implemented in the intrinsic absorption range.

Figure 2 shows the photoluminescence spectra of (a) the CdTe layer in an *n*-CdS/*p*-CdTe heterostructure subjected to frontal excitation without CdS illumination and (b) the CdTe layer formed on a pure glass substrate (from [11]); both CdTe layers were grown under identical technological conditions. Note that, in contrast to single crystals [12] and large-crystallite polycrystals [13, 14], the LTPL spectra of fine-grained films exhibit neither exciton nor DAPs emission. Comparison of the spectra in Figures 2a and 2b show that the presence of a thin polycrystalline CdS layer, which plays a role of a conditional substrate with a heterointerface, is pronounced in only the far edge region.

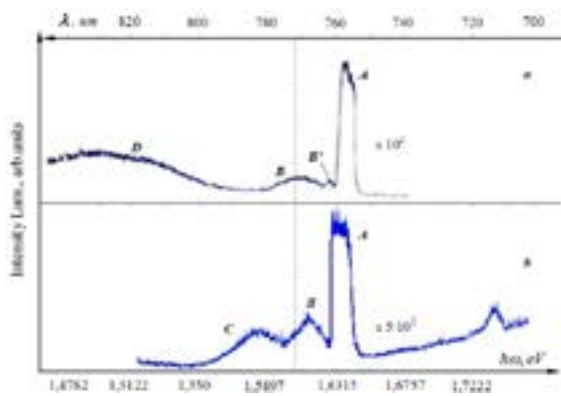


**Figure 2** – Photoluminescence spectra of the CdTe layer (a) in an n-CdS/p-CdTe heterostructure in the absence of CdS illumination and (b) on a pure glass substrate;  $T = 4.2$  K.

The luminescence spectra of these samples in the range of 750–760 nm qualitatively coincide and consist of a dominant  $e-h$  emission band ( $A$  line) with a half-width of  $\Delta E_A \approx 11.2 \pm 0.1$  meV and  $\Delta E_A \approx 14.2 \pm 0.1$  meV, respectively. The sharp long-wavelength edges of the  $A$  lines indicate that the crystallites of the CdTe films grown on both glass and photoresistive substrates have a fairly high bulk structural quality. These edges are shifted above with respect to the bottom of the conduction band (vertical dash-and-dot line) of single crystal at  $T = 4.2$  K ( $E_g = 1.606$  eV) by energies  $\Delta E_r \approx 24.4 \pm 0.1$  meV and  $\Delta E_r \approx 21.4 \pm 0.1$  meV, so that the sum  $\Delta E_r + \Delta E_A = \varphi_0 \approx 35.6 \pm 0.2$  meV remains practically the same for both  $A$  lines. The latter is clearly evidenced by the short-wavelength wings of these lines in Figures 2a and 2b. Hence, the following conclusion can apparently be drawn: the  $\varphi_0$  and  $\varphi = \Delta E_r$  values are nothing more but the heights of the surface potential barrier at the crystallite boundary before and after illumination, and  $\Delta E_A$  is the surface photo-emf, generated by the SCR built-in field (see also [11]). Thus, we have a correlation between the micro photovoltaic property and the intrinsic luminescence of crystallites in thin fine-grained films. Here, we should emphasize the detection of the blue shift of the  $A$ -line red edge [11], which related to the  $e-h$  recombination of the hot photocarriers separated by the electric field of interfacial SCR crystallites; this shift is absent in coarse-grained structures [13, 14].

The spectral dependence of the  $A$ -line intensity can be presented as [11]

$$L(\omega) = A_0(\hbar\omega - E'_g)^{1/2} \exp(-(\hbar\omega - E'_g)/kT_{eh}) \quad (5)$$

where  $A_0$  is a constant, dependent on the type of the film and its photoexcitation conditions;  $E'_g = E_g + \Delta E_r$  is the energy of the  $A$ -line red edge;  $k$  is the Boltzmann constant; and  $T_{eh}$  is the mean characteristic temperature of photocarriers. Obviously, the second and third factors in the right-hand side of (5) are due to the densities of states in the simple quadratic bands and the quasi-equilibrium photocarrier distribution functions.

As can be seen in Figure 2, the luminescence spectrum of the CdTe layer in the n-CdS/p-CdTe heterostructure, in contrast to the spectrum of the CdTe monolayer, does not contain any hot-luminescence region in the wavelength range  $\lambda < 750$  nm; however, it exhibits an additional relatively strong and wide  $D$  line of edge luminescence in the range of 790–870 nm, with a half-width  $\Delta E_D \approx 120$  meV and a maximum at a frequency  $\hbar\omega \approx 1.49$  eV. The energy of this line is lower than  $E_g$  by  $\sim 40$  meV, which is of the same order of magnitude as the  $\Delta E_c$  value (the discontinuity of the CdTe and CdS conduction band bottoms at the heterojunction interface).

Naturally, one would expect the occurrence of the  $D$  line of CdTe edge luminescence in n-CdS/p-CdTe to be due to the contact electric field of the heterojunction, which extracts some part of generated photoelectrons from the p-CdTe layer to the surface region of the n-CdS layer. These transferred electrons relax in energy to reduce the potential barrier of the heterojunction and undergo radiative tunnel recombination with holes from the p-CdTe region or via surface levels  $E_s$  (Figure 3); these processes determine the strong broadening of the  $D$  line, which possesses a long short-wavelength tail and horizontal background. It should be noted that, although the luminescence through the  $D$  channel is related to only the interface and occurs at a depth equal to the p-CdTe layer thickness, it is nevertheless directly correlated by the  $A$  line, because separated photocarriers in the SCR of p-CdTe crystallites contribute to both lines. The quenching of hot luminescence in the spectrum in Figure 2b is also due to the influence of the contact field, possible heterojunction defects, and related crystallite bulk defects on the energy relaxation of hot photocarriers.

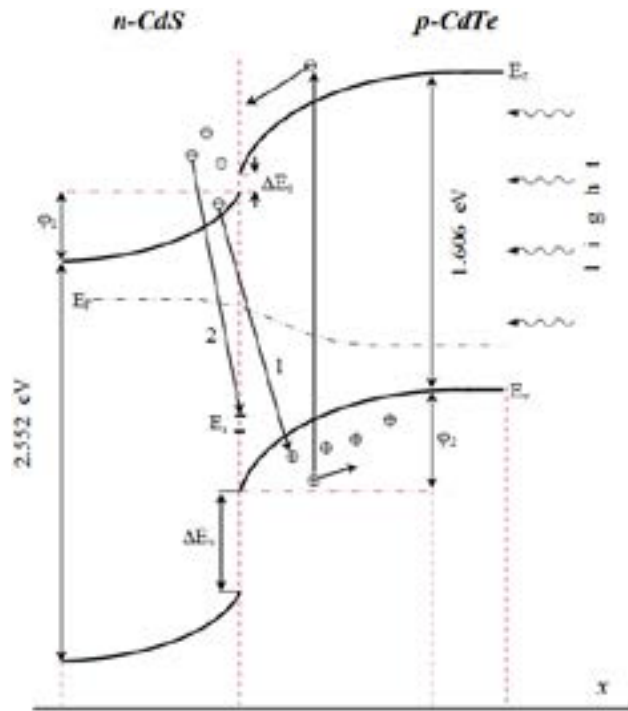


**Figure 3** – Schematic energy band diagram of a sharp n-CdS/p-CdTe heterojunction under illumination from the CdTe side and a schematic diagram of the radiative recombination processes (1, 2) leading to the formation of the luminescence D line;  $T = 4.2$  K.

Figure 2a shows also that the long-wavelength wing of the *A* line with a weak doublet fine structure (*B* and *B'* lines) somewhat differs from the similar structure (*B* and *C* lines) of the CdTe monolayer spectrum. The maxima of the *B* and *B'* lines are located at wavelengths of 770 and 762 nm, respectively, and their intensities are almost an order of magnitude lower than the maximum intensity of the *A* line. The mechanisms of the formation of these lines are rather complex. The *B* and *C* lines are most likely the one- and two-LO-phonon replicas of the *A* line [11], although radiative transitions of the "c-band  $\rightarrow$  shallow acceptor," "shallow donor  $\rightarrow$  v band," and "band  $\rightarrow$  crystallite interface levels" types may contribute to their formation. At the same time, it should be noted that, first, the *A*, *B*, *B'*, and *D* lines in the luminescence spectrum of the *p*-CdTe layer in an

*n*-CdS/*p*-CdTe heterostructure have not been observed previously by other researchers and, second, their formation obviously involves the luminescence emerging from different depths and the contributions of different structural parts (interface, bulk, surface, barrier regions) of the crystallites forming the fine-grained film.

The illumination of CdS with an intensity  $L_{\text{ill}} = 500$  lx leads to a significant transformation of the luminescence spectrum of CdTe layer (Figure 4a). The *A*, *B*, *B'*, and *D* luminescence lines practically disappear. The free-exciton luminescence range of 770–790 nm with a pronounced doublet structure and the DAPs luminescence range of 790.0–820.0 nm can clearly be distinguished. A similar pattern is observed in the reflection spectrum (Figure 4b): the exciton resonance ( $\lambda_{\text{ex}} = 782.5$  nm,  $\hbar\omega_{\text{ex}} = 1.585$  eV) and the DAPs range of 800–812.5 nm.

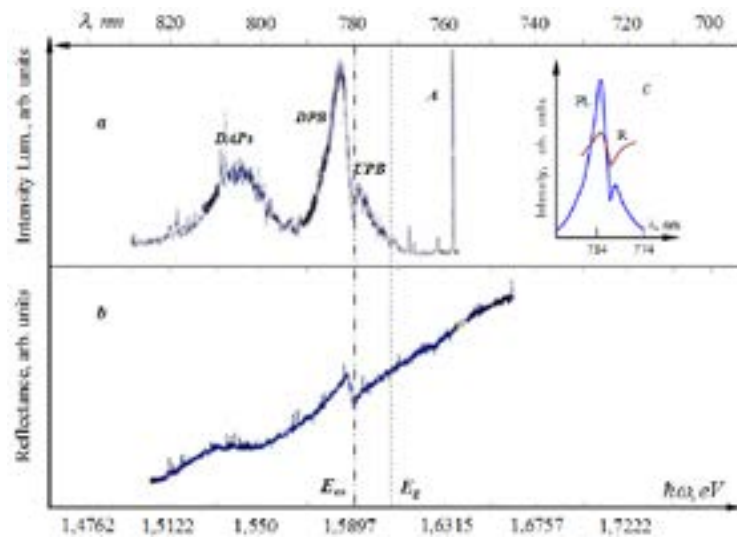


**Figure 4** – (a) Photoluminescence spectra of the CdTe layer in an n-CdS/p-CdTe heterostructure with CdS illumination intensity ( $L_{ill} \approx 500$  lx) and (b) the reflection spectrum of CdTe at  $T = 4.2$  K. The inset in panel a shows the photoluminescence (PL) and specular reflection (R) spectra of a CdTe crystal of stoichiometric composition, recorded at  $T = 77$  K [17].

Naturally, the illumination of the CdS region transforms the n-CdS/p-CdTe heterostructure with frontally excited p-CdTe layer into a state similar to that of short-circuited photocell. Depending on the illumination intensity  $L_{ill}$ , the surface-barrier height decreases and a short-circuit current arises; specifically this current is responsible for the weakening of the  $e-h$  emission (luminescence line A) and other related emission channels (B, B', and D). At a sufficiently high illumination intensity ( $L_{ill} \geq 500$  lx), due to the high photoconductivity of the CdS layer (the condition  $\tau_M < \tau_i$  is implemented), free photocarriers with energies  $\hbar\omega \geq E'_g$  are almost completely involved in the short-circuit current through the heterojunction. In addition, the CdS illumination weakens the contact electric field of the heterojunction (because of the charge exchange in the surface states), as well as the surface potential barriers of crystallites in the p-CdTe layer. As a result, the exciton and impurity Stark effects (which lead to the luminescence build-up in the exciton and DAPs channels) are weakened. Noteworthy features are the symmetric Lorentzian profile of the DAPs luminescence asymmetric doublet structure of the exciton emission.

For comparison, Figure 4c shows the photoluminescence and reflection spectra of a CdTe crystal with a close-to-stoichiometric composition in the vicinity of free exciton at a temperature of 77.3 K, taken from [17-18]. We can see a rather good

qualitative coincidence of two spectral lines, although they were recorded for different crystal structures at different temperatures. The spectrum in Figure 4c is adequately described in terms of the quantum polariton luminescence theory developed in [12] with the following values of the main parameters of the exciton resonance  $A_{n=1}$  in CdTe crystal:  $\hbar\omega_0 = 1.585$  eV,  $\hbar\omega_{LT} = 1.0$  meV,  $\hbar\Gamma = 0.62$  meV,  $M_{ex} = 0.5m_0$  ( $m_0$  is the free-electron mass), background permittivity  $\epsilon_b = 9.65$ , and "dead layer" thickness  $l = 75$  Å. The 11-meV red shift of the exciton resonance in the polycrystalline CdTe film under study is explained by the strong damping of mechanical excitons  $\hbar\Gamma$ , which is caused by the scattering from impurities and grain-boundary potential barriers. Thus, the doublet structure of the exciton luminescence in Figure 4a is described within the polariton model [12-15]. The stronger long-wavelength component peaking at a frequency  $\hbar\omega_d = 1.584$  eV corresponds to the lower branch polariton emission, and the decisive contribution to the weaker blue satellite peaking at  $\hbar\omega_u = 1.590$  eV is from the upper branch polariton emission. The dip ("longitudinal") frequency  $\hbar\omega_L = 1.588$  eV determines the minimum energy of longitudinal excitons.

The symmetric DAPs luminescence profile peaking at the frequency  $\hbar\omega_{DA} = 1.540$  eV ( $\lambda = 805$  nm) has a half-width  $\hbar\Delta\omega_{DA} = 33$  meV and, in contrast to the spectra of pure crystals [14-19] and the spectra recorded without CdS illumination (Figure

2b), does not contain any inhomogeneous broadening due to the LO replicas. The transitions in a DAPs formed by a shallow donor and a shallow acceptor, whose activation energy is  $E_g - \hbar\omega_{DA} = 1.606 - 1.540 = 0.066$  eV, is responsible for this profile, while the strong homogeneous broadening is due to the strong donor–acceptor interaction in the field of grain boundary potential barriers (and, correspondingly, as a result of the formation of DAPs clusters). The DAPs luminescence occurs mainly in the crystallite barrier regions and in the heterojunction (the CdTe region where photocarriers are separated and, therefore, radiative  $e-h$  transitions barely exist). The grain boundary potential barriers and donor–acceptor interactions are responsible for the homogeneous broadening of the DAPs emission line.

### Conclusions

Thus, using illumination ( $L_{\text{ill}} \approx 5 \times 10^2$  lx) of the CdS layer in an  $n$ -CdS/ $p$ -CdTe heterostructure, we could detect polariton and shallow-DAPs emission lines from the thin fine-grained CdTe layer. At low illumination levels ( $L_{\text{ill}} \leq 5 \times 10^2$  lx), they cannot be

clearly selected against the background of the stronger band-to-band emission of the photocarriers separated by the intercrystallite energy field of the high-resistivity polycrystal. The illumination of the CdS layer reduces its shunting resistance, and, correspondingly, the Maxwell relaxation time of separated photocarriers in the crystallite bulk, due to which the photocarriers are pulled in by the heterojunction field before recombining radiatively. Specifically, this circumstance leads to the quenching of the emission lines detected in the absence of illumination and the build-up of the free-exciton and shallow-DAPs lines under illumination.

The  $n$ -CdS/ $p$ -CdTe structure elaborated in this work opens new prospects for not only its practical application as a light converter but also for developing new methods of studying photoelectric phenomena in semiconductor micro- and nanostructures.

### Acknowledgments

Authors thank the staff of the scientific research laboratory of the Ferghana Polytechnic Institute and the professor of the department of the "Physics" N.Kh. Yuldashev for their scientific advice.

### References

1. Tuteja M., Koirala P., Soares J., Collins R., Rockett A. "Low temperature photoluminescence spectroscopy studies on sputter deposited CdS/CdTe junction and solar cells" *Journal of Materials Research* 31(02).(2016):186.
2. Polvonov B.Z., Nasirov M.X., Mirzaev V.T., Razikov J. "Diagnostika poluprovodnikovix materialov metodom polyaritonnoy lyuminessensii" *General question of world science Collection of scientific papers on materials VII International Scientific Conference. Izdatelstvo:"Nauka Rossii" 2.(2019):39*
3. Caraman I., Vatavu S., Rusu G., Gasin P. "The luminescence of CdS and CdTe thin films, components of photovoltaic cells", *Chalcogenide Letters* 3(1).(2006):7.
4. Ikhmayies Sh. J., Ahmad-Bitar R. N. "Interface photoluminescence of the SnO<sub>2</sub>:F/CdS:In/CdTe thin film solar cells prepared partially by the spray pyrolysis technique" *Journal of Luminescence* 132(02).(2012):502.
5. Akhmadaliev B.J., Mamatov O.M., Polvonov B. Z., Yuldashev N.Kh. "Low-temperature photoluminescence of fine-grained CdTe layer in  $n$ -CdS/ $p$ -CdTe film heterostructure" *International Journal of Modern Physics and Application* 4(5).(2017):28
6. Nakamura K., Gotoh M., Fujihara T., Toyama T., and et al. "Electromodulated Photoluminescence Study of CdS/CdTe Thin-Film Solar Cell" *Japanese Journal of Applied Physics* 40(1).(2001):4508.
7. Potter M.D., Halliday D.P., Cousins M., Durose K. "Study of the effects of varying cadmium chloride treatment on the luminescent properties of CdTe/CdS thin film solar cells" *Thin Solid Films* 361–362, (2000):248.
8. Kosyachenko L.A., Savchuk A.I., Grushko E.V. "Influence of a thickness of an absorbing layer on efficiency of CdS/CdTe solar cells" *Semiconductors* 43(8). (2009):1060.
9. Ilchuk G.A., Kusnej V.V., Rud V.Yu., Rud Yu.V., Shapoval P.Y., Petrus R.Y. "Photosensitivity of  $n$ -CdS/ $p$ -CdTe heterotransitions received by chemical superficial sedimentation" *Semiconductors* 44(3).(2010):335.
10. Tuteja M. "Low temperature photoluminescence studies on sputter deposited cadmium sulphide/cadmium telluride heterojunctions and solar sells" *Thesis. University of Illinois at Urbana-Champaign* 31(02). (2014):24.
11. Akhmadaliev B.J., Mamatov O.M., Polvonov B.Z., Yuldashev N.Kh. "Correlation Between the Low-Temperature Photoluminescence Spectra and Photovoltaic Properties of Thin Polycrystalline CdTe Films" *JAMP (USA)* 4(02). (2016):391.

12. Akhmadaliev B.J., Polvonov B.Z., Yuldashev N.Kh. "Influence of Exciton Decay on the Polariton Luminescence Spectra of CdTe Crystal" *Journal of Optics and Spectroscopy* 116(02). (2014):244.
13. Ushakov V.V., Klevkov Yu.V., Dravin V.A. "Ion implantation Er in polycrystalline cadmium telluride", *Semiconductors* 49(5).(2015):644.
14. Bagaev, V.S., Klevlov, Yu.V., Kolosov, S.A., Krivobok, V.S., Shepeli, A.A. "Optical and electrophysical properties of defects in high-purity CdTe" *Physics of the Solid State* 52(01).(2010):37.
15. Polvonov B.Z., Yuldashev N.K. Nasirov M.H., Mirzarakhimova F.K. "Diagnostics of semiconductor materials such as cadmium chalcogenides by the method of low-temperature polariton luminescence" *Journal of International Scientific Review, Boston, USA* 11(53).(2018):24.
16. Polvonov B.Z., Yuldashev N.K. "The photo voltage film p-CdTE with the photo responsive-operated substrate n-CdS" *The Third European Conference on Physics and Mathematics, Vienna, Austria.* (2015).12.
17. Akhmadaliev B.J., Mamatov O.M., Polvonov B. Z., Yuldashev N.Kh. "Low-temperature photoluminescence of fine-grained CdTe layer in n-CdS/p-CdTe film heterostructure" *International Journal of Modern Physics and Application* 4(5).(2017):28.
18. Akhmadaliev B.J., Polvonov B.Z., Yuldashev N.Kh. "Influence of Exciton Decay on the Polariton Luminescence Spectra of CdTe Crystal " *Optics and Spectroscopy* 116 (02).(2014):244.
19. Polvonov B.Z., Nasirov M.X., Polvonov O.Z., Tuychibaev B.K. "Osobennosti povisheniya moshnosti fotovoltaicheskix plenochnix struktur xalkogenidov kadmiya" *Oriental renaissance: Innovative, educational, natural and social sciences* 1(11).(2021):1046

© This is an open access article under the (CC)BY-NC license (<https://creativecommons.org/licenses/by-nc/4.0/>).  
Funded by Al-Farabi KazNU.